The Fuzzy Neural Network Control Scheme With H_∞ Tracking Characteristic of Space Robot System With Dual-arm After Capturing a Spin Spacecraft

Jing Cheng and Li Chen

***Abstract*—In this paper, the dynamic evolution for a dual-arm space robot capturing a spacecraft is studied, the impact effect and the coordinated stabilization control problem for post-impact closed chain system are discussed. At first, the pre-impact dynamic equations of open chain dual-arm space robot are established by Lagrangian approach, and the dynamic equations of a spacecraft are obtained by Newton-Euler method. Based on the results, with the process of integral and simplify, the response of the dual-arm space robot impacted by the spacecraft is analyzed by momentum conservation law and force transfer law. The closed chain system is formed in the post-impact phase. Closed chain constraint equations are obtained by the constraints of closed-loop geometry and kinematics. With the closed chain constraint equations, the composite system dynamic equations are derived. Secondly, the recurrent fuzzy neural network control scheme is designed for calm motion of unstable closed chain system with uncertain system parameter. In order to overcome the effects of uncertain system inertial parameters, the recurrent fuzzy neural network is used to approximate the unknown part, the control method with H_∞ tracking characteristic. According to the Lyapunov theory, the global stability is demonstrated. Meanwhile, the weighted minimum-norm theory is introduced to distribute torques guarantee that cooperative operation between manipulators. At last, numerical examples simulate the response of the collision, and the efficiency of the control scheme is verified by the simulation results.**

***Index Terms*—Capturing operation, calm motion control, closed chain system, dual-arm space robot, recurrent fuzzy neural network, H_∞ tracking characteristic.**

I. Introduction

AS the exploration of space continuously advancing, the space robot has been employing to accomplish more on-orbit service missions [1]. There is harsh operating environment in outer space, space robot system assisted astronauts complete space missions, can protect the astronauts' life from dangers. Space robotic systems have received a large number of significant attentions [2]−[5] in the past decades. The space robot was employed to accomplish complicated tasks, such as fueling, maintaining of spacecraft in earth orbit, clearing of orbital debris, etc. [6]−[8]. Therefor it is becoming increasingly important for space robot system to have the capability of capturing a satellite. As space robot system with dual-arm possesses bigger carrying capacity and better structure rigidity, it is more expected to fulfil capturing spacecraft tasks. Since the weightlessness condition in outer space, it makes the dynamics and control problems related to capturing satellite operation by space robot system with dual-arm to be extremely complicated compared with the counterpart of fixed-base robot system and single arm space robot system, and there are some unique characteristics, such as, nonholonomic dynamics restriction, change of system configuration, transfer of linear momentum, angular momentum and energy, topology transfer from open to closed loop system, and the constraints of closed-loop geometry and kinematics during capturing satellite operation. It develops many challenging problems that need to be solved.

Space robot system is essentially a coupling, time-varying and nonlinear system [9]−[11], if there is uncertain parameter exists in the system will make control scheme design more difficult [12], [13]. Vafa *et al.* [14] proposed a concept of virtual manipulator approach for the kinematics and dynamics analysis of space robot. Nakamura *et al.* [15] proposed a concept of generalized Jacobi matrix, and studied the relation between the velocity of joint space and the velocity of working space for single arm space robot. Huang *et al.* [16]−[18] studied the application of tethered space robots capturing a target in future on-orbit missions, they analyzed the impact dynamic modeling and proposed coordinated stabilization scheme, adaptive postcapture backstepping control, *et al.* for tumbling tethered space robot-target combination. Abad *et al.* [19] predicted the best capturing time and configuration of the target, and found an optimal control solution to guide the robot to reach the predicted location with a minimal attitude disturbance. Rekleitis *et al.* [20] proposed a planning and control methodology for manipulating passive objects by cooperating orbital free-flying servicers in zero gravity.

During the process of capturing operation, the end-effectors of dual-arm space robot will inevitably collide with the captured target. The collision lead to instability and rolling of space robot in the weightlessness environment which is harm for the precise instrument on the servicing spacecraft, even lead to the failure of space missions. Because of the aforementioned challenging problems, the current studies are mostly focus on single arm space robot [21]−[23]. In fact, dual-arm space robot is similar to human arms; it is more suitable for capturing operation. Patolia *et al.* [24] discussed the coordinated motion planning problems for the dual-arm space robot system. Chen *et al.* [25] proposed an hybrid position and force control method based on radial basis function

This work was supported by the National Natural Science Foundation of China (11372073, 11072061). Recommended by Associate Editor Yuanqing Xia. *(Corresponding author: Jing Cheng.)*

Citation: J. Cheng and L. Chen, "The fuzzy neural network control scheme with H_∞ tracking characteristic of space robot system with dual-arm after capturing a spin spacecraft," *IEEE/CAA J. Autom. Sinica*, vol. 7, no. 5, pp. 1417−1424, Sept. 2020.

J. Cheng is with the School of Aerospace Engineering, Tsinghua University, Beijing 100084, China (e-mail: chengjingf@mail.tsinghua.edu.cn).

L. Chen is with the School of Mechanical Engineering and Automation, Fuzhou University, Fuzhou 350116, China (e-mail: chnle@fzu.edu.cn).

Digital Object Identifier 10.1109/JAS.2018.7511180

neural network for a closed chain space robot. Shah *et al.* [26] found the optimal motion planning strategy for dual-arm space robot to reduce the influence of capturing operation. Aforementioned studies give primary attention to trajectory planning and control of dual-arm space robot in pre-impact phase, none of them have considered that impact effort and calm control method for the composite system with closed chain after the collision.

This paper is devoted to dynamic evolution analysis of dual-arm space robot capturing a spin spacecraft, and the impact effort and control scheme of the closed chain with uncertain inertial parameters are discussed. First, based on the Lagrangian approach and Newton-Euler method, the pre-impact dynamic models of dual-arm space robot and a spin spacecraft are established respectively. The dual-arm space robot and the spacecraft form a closed chain system in the post-impact phase. According to the closed chain constraint equations, the dynamic equations of the closed chain system are obtained. The impact effect of closed chain system after the collision analyzed by momentum conservation law and force transfer law. Then, for the unstable closed chain system with uncertain system parameter, the recurrent fuzzy neural network control scheme is designed for calm motion. The recurrent fuzzy neural network is used to approximate the unknown part of the system [27], [28]. For the approximate error, the control scheme which is satisfied the H_∞ performance indicators requirement [29], [30]. The stability of the system with H_∞ tracking characteristic is demonstrated according to Lyapunov theory. For the existence of the controller redundancy, The introduction of the weighted minimum-norm theory is applied to distribute the torques harmoniously of each joint. Finally, the numerical examples simulate the response of collision for closed chain system and confirm that the proposed control scheme is reliable for the calm motion of unstable system.

II. Dynamic Evaluation Analysis for Dual-Arm Space Robot Capturing a Spacecraft

The dual-arm space robot and target spacecraft are is shown in Fig. 1.

The dual-arm space robot system consists of a floating rigid base, two manipulator arms, each arm have three links. The target spacecraft is a rigid body. The inertia coordinate inertial coordinate frames XOY is built, origin O is located at an arbitrary point in the plane. $x_iO_iy_i(i=1,2,\ldots,6)$ is the local frame coordinate of base or each link. O_0 and O_l are the mass center of base and load; $O_i(i=1,2,\ldots,6)$ is the mass center of each link. $l_i(i=1,2,\ldots,6)$ is the length of each link. The length of $\overline{O_0O_1}$ and $\overline{O_0O_4}$ are d_0. The distance of mass center O_l of load to left end-effector and right end-effector are d_L and d_R respectively. $m_i(i=1,2,\ldots,6)$ is the mass of ith link. m_0 and m_l represent the mass of base and load respectively. $I_i(i=1,2,\ldots,6)$ is the center inertial moment of ith link. I_0 and I_l represent the center inertial moment of base and load respectively. ψ_1 is the angle measured counterclockwise from the positive x_0-axis to $\overline{O_0O_1}$. ψ_2 is the angle between x_0-axis and $\overline{O_0O_4}$. ψ_1 and ψ_2 are constant values.

We denote $\boldsymbol{q}=[x_0\ \ y_0\ \ \theta_0\ \ \boldsymbol{\theta}_L^T\ \ \boldsymbol{\theta}_R^T]^T$ as generalized coordinates of dual-arm space robot and neglect the microgravity, the pre-impact dynamic equations of dual-arm space robot are derived by using Lagrangian equations as

$$\boldsymbol{M}(\boldsymbol{q})\ddot{\boldsymbol{q}}+\boldsymbol{H}(\boldsymbol{q},\dot{\boldsymbol{q}})\dot{\boldsymbol{q}}=\begin{bmatrix}\boldsymbol{0}_{2\times1}\\ \boldsymbol{\tau}\end{bmatrix}+\boldsymbol{J}^T\boldsymbol{F} \tag{1}$$

where $\boldsymbol{M}(\boldsymbol{q})\in\mathbb{R}^{9\times9}$ is the symmetric positive mass matrix, $\boldsymbol{H}(\boldsymbol{q},\dot{\boldsymbol{q}})\dot{\boldsymbol{q}}\in\mathbb{R}^{9\times1}$ contains the Coriolis and centrifugal force. The $\boldsymbol{\tau}=[\boldsymbol{\tau}_B^T\ \ \boldsymbol{\tau}_L^T\ \ \boldsymbol{\tau}_R^T]^T$ is the generalized control torque, $\boldsymbol{\tau}_B$ is the control force/torque of base, vectors of $\boldsymbol{\tau}_L$ and $\boldsymbol{\tau}_R$ represent the control torques of left manipulator and right manipulator. $\boldsymbol{F}\in\mathbb{R}^{6\times1}$ is the impact force acts on the end-effectors of manipulators. $\boldsymbol{J}\in\mathbb{R}^{6\times9}$ is corresponding motion Jacobi matrix.

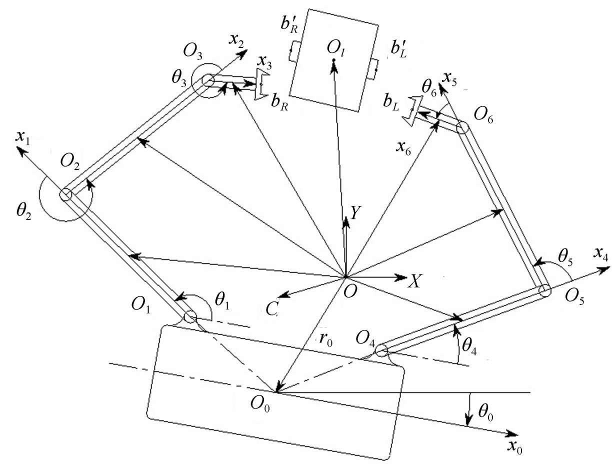

Fig. 1. Dual-arm space robot system and target system in pre-impact phase.

According to the geometric relations, the relationship between the velocity of end-effectors and coordinates can be expressed as

$$\boldsymbol{s}_b=\boldsymbol{J}\dot{\boldsymbol{q}} \tag{2}$$

where $\boldsymbol{s}_b=[\dot{x}_{bL}\ \ \dot{y}_{bL}\ \ \dot{\theta}_{bL}\ \ \dot{x}_{bR}\ \ \dot{y}_{bR}\ \ \dot{\theta}_{bR}]^T$.

Vector $\boldsymbol{q}_l=[x_l\ \ y_l\ \ \theta_l]^T$ is represent the location of the mass center and base attitude which is defined as generalized coordinates for target spacecraft. The dynamic equations of the target can be derived base on the Newton-Euler formulation

$$\boldsymbol{D}_l\ddot{\boldsymbol{q}}_l=\boldsymbol{J}_l^T\boldsymbol{F}' \tag{3}$$

where $\boldsymbol{D}_l\in\mathbb{R}^{3\times3}$ is the symmetric positive inertial matrix, $\boldsymbol{F}'$ is counter-acting forces.

Touch points b'_L and b'_R are located on the target which will connect with end-effectors after capture operation. Similarly with (2), the relationship between the velocity of touch points and coordinates can be expressed as

$$\boldsymbol{s}_{b'}=\boldsymbol{J}_l\dot{\boldsymbol{q}}_l \tag{4}$$

where $\boldsymbol{s}_{b'}=[\dot{x}_{b'L}\ \ \dot{y}_{b'L}\ \ \dot{\theta}_{b'L}\ \ \dot{x}_{b'R}\ \ \dot{y}_{b'R}\ \ \dot{\theta}_{b'R}]^T$, $\boldsymbol{J}_l=[\boldsymbol{J}_{lL}^T\ \ \boldsymbol{J}_{lR}^T]^T$ is corresponding motion Jacobi matrixes, $\boldsymbol{J}_{lL},\boldsymbol{J}_{lR}\in\mathbb{R}^{3\times3}$.

According to Newton's third law, we have

$$\boldsymbol{F}'=-\boldsymbol{F}. \tag{5}$$

Impact forces can be decomposed as follow:

$$\boldsymbol{F}'=(\boldsymbol{J}_l^T)^{+}\boldsymbol{M}_l\ddot{\boldsymbol{q}}_l+\boldsymbol{F}_I \tag{6}$$

where $(\boldsymbol{J}_l^T)^+$ is the Moore-Penrose pseudo-inverse of $\boldsymbol{J}_l^T$. $(\boldsymbol{J}_l^T)^+\boldsymbol{M}_l\ddot{\boldsymbol{q}}_l$ is operating force item. $\boldsymbol{F}_I$ represents tensile force or pressure force on the target, and $\boldsymbol{J}_l^T\boldsymbol{F}_I = 0$.

Invoking (3), (4), (5), and (6), we can obtain that

$$\boldsymbol{M}(\boldsymbol{q})\ddot{\boldsymbol{q}} + \boldsymbol{H}(\boldsymbol{q},\dot{\boldsymbol{q}})\dot{\boldsymbol{q}} = \boldsymbol{\tau} - \boldsymbol{J}^T(\boldsymbol{J}_l^T)^+\boldsymbol{M}_l\ddot{\boldsymbol{q}}_l - \boldsymbol{J}^T\boldsymbol{F}_I. \quad (7)$$

Integrating (7) over the momentary period of collision

$$\int_{t_0}^{t_0+\Delta t}[\boldsymbol{M}(\boldsymbol{q})\ddot{\boldsymbol{q}} + \boldsymbol{H}(\boldsymbol{q},\dot{\boldsymbol{q}})\dot{\boldsymbol{q}}]dt = \int_{t_0}^{t_0+\Delta t}\left[\boldsymbol{\tau} - \boldsymbol{J}^T(\boldsymbol{J}_l^T)^+\boldsymbol{M}_l\ddot{\boldsymbol{q}}_l - \boldsymbol{J}^T\boldsymbol{F}_I\right]dt. \quad (8)$$

The period of impact is transient: $\Delta t \to 0$. The generalized coordinates is approximated as constant value, and the generalized velocity is changed in a limited range. There is no input torques during the momentary period of collision. Besides, the impact force is huge so that $\boldsymbol{F}_I$ [31] can be ignored. According to the theorem of impulse, (8) can be further reformulated as

$$\boldsymbol{M}\left[\dot{\boldsymbol{q}}(t_0+\Delta t) - \dot{\boldsymbol{q}}(t_0)\right] + \boldsymbol{J}^T\left[(\boldsymbol{J}_l^T)^{-1}\boldsymbol{M}_l(\dot{\boldsymbol{q}}_l(t_0+\Delta t) - \dot{\boldsymbol{q}}_l(t_0))\right] = 0. \quad (9)$$

Target and end-effectors are fixedly connected after the capturing operation, the whole system can be regard as a composite system with closed chain.

Denote $\boldsymbol{q}_f = [x_0 \quad y_0 \quad \theta_0 \quad \boldsymbol{\theta}_L^T]^T$, consider the geometric relations of left arm and target, we have

$$\boldsymbol{J}_L\dot{\boldsymbol{q}}_f(t) = \boldsymbol{J}_{lL}\dot{\boldsymbol{q}}_l(t). \quad (10)$$

In order to obtain the constraint equations of the closed chain system, the composite system is cut at point b_L which is shown in Fig. 2. Since cut points have the same movement velocity and angular velocity, relationship of left arm angles and right arm angles reference to base-fix coordinate $x_0O_0y_0$ can be derived as

$$\boldsymbol{G}_L\dot{\boldsymbol{\theta}}_L = \boldsymbol{G}_R\dot{\boldsymbol{\theta}}_R \quad (11)$$

where $\boldsymbol{G}_L = [\boldsymbol{J}_{0L}^T \ \ \boldsymbol{I}_{3\times1}]^T$, $\boldsymbol{G}_R = [\boldsymbol{J}_{0R}^T \ \ \boldsymbol{I}_{3\times1}]^T$, $\boldsymbol{J}_{0L} \in \mathbb{R}^{2\times3}$, $\boldsymbol{J}_{0R} \in \mathbb{R}^{2\times3}$ are corresponding motion Jacobi matrixes of the cut points reference to base-fix coordinate $x_0O_0y_0$.

Noting that

$$\boldsymbol{U} = [\boldsymbol{I}_{6\times6} \quad \boldsymbol{U}_1^T] \quad (12)$$

$$\boldsymbol{U}_1 = [\boldsymbol{O}_{3\times3} \quad \boldsymbol{G}_{\mathrm{R}}^{-1}\boldsymbol{G}_L] \quad (13)$$

where $\boldsymbol{I}_{n\times n}$ is a $n\times n$ unit matrix, $\boldsymbol{O}_{n\times n}$ is a $n\times n$ zero matrix.

With the (11), (12), and (13) we have

$$\dot{\boldsymbol{q}} = \boldsymbol{U}^T\dot{\boldsymbol{q}}_f. \quad (14)$$

Solving (9), the response of composite system is obtained

$$\dot{\boldsymbol{q}}_f(t_0+\Delta t) = \boldsymbol{L}^{-1}\left[\boldsymbol{R}\dot{\boldsymbol{q}}_f(t_0) + \boldsymbol{U}\boldsymbol{J}^T(\boldsymbol{J}_l^T)^+\boldsymbol{M}_l\dot{\boldsymbol{q}}_l(t_0)\right] \quad (15)$$

where $\boldsymbol{L} = \boldsymbol{R} + \boldsymbol{U}\boldsymbol{J}^T(\boldsymbol{J}_l^T)^+\boldsymbol{M}_l\boldsymbol{J}_{lL}^{-1}\boldsymbol{J}_L$, $\boldsymbol{R} = \boldsymbol{U}\boldsymbol{M}\boldsymbol{U}^T$.

Differentiating (13), we can obtain that

$$\ddot{\boldsymbol{q}} = \boldsymbol{U}^T\ddot{\boldsymbol{q}}_f + \dot{\boldsymbol{U}}^T\dot{\boldsymbol{q}}_f. \quad (16)$$

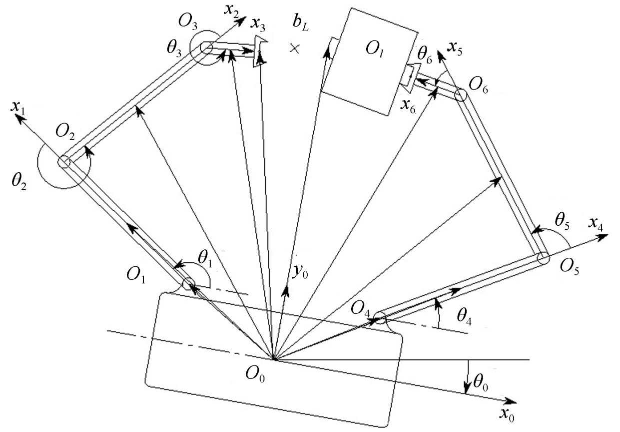

Fig. 2. Closed chain system in pre-impact phase with virtual cut-point.

Substituting (14), and (16) into (7), we have

$$\bar{\boldsymbol{M}}\ddot{\boldsymbol{q}}_f + \bar{\boldsymbol{H}}\dot{\boldsymbol{q}}_f = \boldsymbol{U}\boldsymbol{\tau} - \boldsymbol{U}\boldsymbol{J}^T\boldsymbol{F}_I \quad (17)$$

where $\bar{\boldsymbol{M}} = \boldsymbol{R} + \boldsymbol{U}\boldsymbol{J}^T(\boldsymbol{J}_l^T)^+\boldsymbol{M}_l\boldsymbol{J}_{lL}^{-1}\boldsymbol{J}_L$, $\bar{\boldsymbol{H}} = \boldsymbol{U}[\boldsymbol{H}\boldsymbol{U}^T + \boldsymbol{M}\dot{\boldsymbol{U}}^T] + \boldsymbol{U}\boldsymbol{J}^T(\boldsymbol{J}_l^T)^+\boldsymbol{M}_l\boldsymbol{J}_{lL}^{-1}(\dot{\boldsymbol{J}}_L - \dot{\boldsymbol{J}}_{lL}\boldsymbol{J}_{lL}^{-1}\dot{\boldsymbol{J}}_L)$.

The dynamic model of unstable closed chain system with closed-loop constraints has been obtained so far. The unstable motion is harm for the space equipment, it is necessary to propose a proper control scheme for the calm motion of whole system.

III. Recurrent Fuzzy Neural Network Control for Closed Chain System With H_∞ Tracking Characteristic

A. Recurrent Fuzzy Neural Network

The neural network [32] and fuzzy logic [33] have their advantages, the learning ability of neural network is used to adjust the fuzzy control by combine neural network with fuzzy control [34], [35]. The neural network has characteristics, and the relationship between input and output of the controller is expressed quantificationally by adjusting the parameters continually to complete control purpose; the fuzzy logical system is dependent on expert experience qualitatively. The fuzzy neural network has combined the advantages of fuzzy neural network and fuzzy logical system and but also overcomes some disadvantages of them. This kind of combination characterized the fuzzy control as self-learning and the neural network as reasoning. In this paper, the neural network is used to realize fuzzy reasoning to constitute the fuzzy neural network control scheme and realize trajectory control. The four-layer recurrent fuzzy neural network which includes input layer, member function layer, rules layer, and output layer is shown in Fig. 3.

Input layer:

$$In_i^{(1)} = Out_i^{(1)} = x_i, \quad i = 1, 2, \ldots, m \quad (18)$$

superscript is corresponding to the layer input and layer output.

Member function layer: Gauss function is chosen as membership function, a_{ij} and b_{ij} are center value and base width of jth language set.

$$Out_{ij}^{(2)} = \mu(Out_i^{(1)}) = e^{-[(Out_i^{(1)} - a_{ij}^2)/b_{ij}^2]}. \quad (19)$$

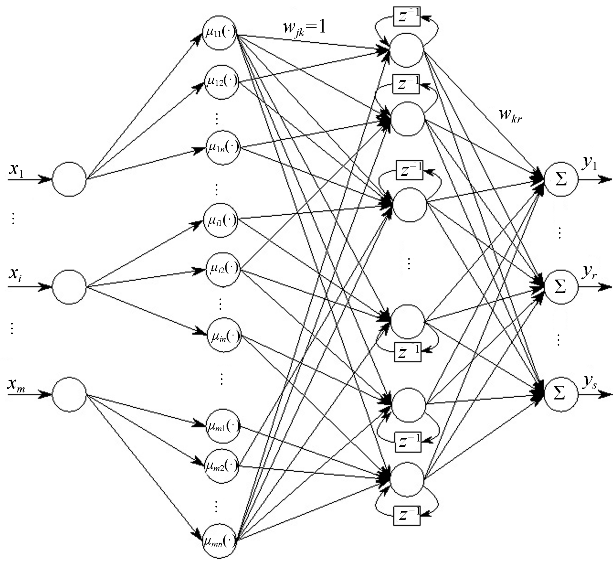

Fig. 3. Structure of recurrent fuzzy neural network.

Fuzzy reasoning layer:

$$Out_k^{(3)} = \prod w_{jk} In_j^{(3)} w_k Out_{k-1}^{(3)}, \quad k = 1, 2, \ldots, u \tag{20}$$

where $In_j^{(3)}$ is the jth input w_{jk} is weight between member function layer and reasoning layer. u is the number of rules.

Output layer: the layer of defuzzification:

$$y_r = Out_r^{(4)} = w_{kr} In_k^{(4)}, \quad r = 1, 2, \ldots, s \tag{21}$$

where $In_k^{(4)}$ is the kth input of this layer, w_{kr} is linked weight between kth rule and output nodes, which is self-turning in the learning process.

Output can be written as follow:

$$u = \boldsymbol{W}_r^T \boldsymbol{\Phi} \tag{22}$$

where $\boldsymbol{W}_r = [w_{1r} \quad w_{2r} \quad \ldots \quad w_{lr}]^T$ is a vector of weights, $\boldsymbol{\Phi} = [x_1 \quad x_2 \quad \ldots \quad x_u]^T$ is the corresponding vector of basis functions.

The recurrent fuzzy neural network feedback unit memorize the previous rules, therefore, the network has characteristics of dynamic nature and simple configuration.

B. Control Design for Closed Chain System

Noting that

$$\bar{\boldsymbol{\tau}} = \boldsymbol{U}\boldsymbol{\tau}, \quad \bar{\boldsymbol{F}}_I = \boldsymbol{U}\boldsymbol{J}^T \boldsymbol{F}_I \tag{23}$$

$\bar{\boldsymbol{\tau}}$ can be rewritten as follow

$$\bar{\boldsymbol{\tau}} = [\bar{\boldsymbol{\tau}}_{\rm a}^T \quad \bar{\boldsymbol{\tau}}_{\rm b}^T]^T \tag{24}$$

where $\bar{\boldsymbol{\tau}}_{\rm a}, \bar{\boldsymbol{\tau}}_{\rm b} \in \mathbb{R}^{3\times 1}$.

Substituting (12) into (23), we have

$$\bar{\boldsymbol{\tau}}_{\rm a} = \boldsymbol{\tau}_B \tag{25}$$

$$\boldsymbol{\Omega}[\boldsymbol{\tau}_L^T \quad \boldsymbol{\tau}_R^T]^T = \bar{\boldsymbol{\tau}}_b \tag{26}$$

where $\boldsymbol{\Omega} = [\boldsymbol{I}_{3\times 3} \quad (\boldsymbol{G}_R^{-1}\boldsymbol{G}_L)^T]$.

The internal force have no influence on closed chain system, the elements in the vector $\bar{\boldsymbol{F}}_I$ are zeros which can be obtained by means of matrix calculating. The reduced-order form of dynamic equation for composite system are reformulated as follow

$$\bar{\boldsymbol{M}}\ddot{\boldsymbol{q}}_f + \bar{\boldsymbol{H}}\dot{\boldsymbol{q}}_f = \bar{\boldsymbol{\tau}}. \tag{27}$$

In order to control the position and attitude of both the base and the load, the output matrix of system is defined as

$$\boldsymbol{X} = [x_0 \quad y_0 \quad \theta_0 \quad x_l \quad y_l \quad \theta_l]^T. \tag{28}$$

Differentiating (28) yields

$$\dot{\boldsymbol{X}} = \boldsymbol{J}_0(\boldsymbol{q}_f)\dot{\boldsymbol{q}}_f \tag{29}$$

where $\boldsymbol{J}_0(\boldsymbol{q}_f) \in \mathbb{R}^{6\times 6}$ is the Jacobian matrix.

Defining the output error as follow

$$\boldsymbol{e} = \boldsymbol{X}_{\rm d} - \boldsymbol{X} \tag{30}$$

where the desired trajectory $\boldsymbol{X}_{\rm d}$ is bounded and continuous.

Substituting (29) into (27) the dynamic equations of closed chain system can be rewritten as:

$$\bar{\boldsymbol{M}}_X\ddot{\boldsymbol{X}} + \bar{\boldsymbol{H}}_X\dot{\boldsymbol{X}} = \bar{\boldsymbol{\tau}} \tag{31}$$

where $\bar{\boldsymbol{M}}_X = \bar{\boldsymbol{M}}\boldsymbol{J}_0^{-1}$, $\bar{\boldsymbol{H}}_X = \bar{\boldsymbol{H}}\boldsymbol{J}_0^{-1} - \bar{\boldsymbol{M}}\boldsymbol{J}_0^{-1}\dot{\boldsymbol{J}}_0\boldsymbol{J}_0^{-1}$.

Since fuel consumption and the other technology factors of space robot, it is very difficult to obtain the exact dynamic model of space robot. Considering the uncertain parameters of system, (31) can be further reformulated as

$$\hat{\bar{\boldsymbol{M}}}_X\ddot{\boldsymbol{X}} + \hat{\bar{\boldsymbol{H}}}_X\dot{\boldsymbol{X}} + \chi = \bar{\boldsymbol{\tau}} \tag{32}$$

where $\boldsymbol{\chi} = \Delta\boldsymbol{M}_X\ddot{\boldsymbol{X}} + \Delta\boldsymbol{H}_X\dot{\boldsymbol{X}}$, $\Delta\boldsymbol{M}_X$, $\Delta\boldsymbol{H}_X$ are modeling errors, $\Delta\boldsymbol{M}_X = \bar{\boldsymbol{M}}_X - \hat{\bar{\boldsymbol{M}}}_X$, $\Delta\boldsymbol{H}_X = \bar{\boldsymbol{H}}_X - \hat{\bar{\boldsymbol{H}}}_X$. $\hat{\bar{\boldsymbol{M}}}_X$, and $\hat{\bar{\boldsymbol{H}}}_X$ are estimated inertia parameter matrices.

Using recurrent fuzzy neural network to approximate the unknown part, $\boldsymbol{\chi}$ can be expressed as

$$\boldsymbol{\chi} = \boldsymbol{W}^{*T}\boldsymbol{\Phi} + \Delta\boldsymbol{\delta} \tag{33}$$

where $\boldsymbol{W}^*$ is the optimal weight matrix. $\boldsymbol{\Phi}$ is a column correlation with basis function, $\Delta\boldsymbol{\delta}$ is approximate error.

For the unstable composite system with uncertain inertial parameters, the control law is given as

$$\boldsymbol{\tau} = \hat{\bar{\boldsymbol{M}}}_X(\ddot{\boldsymbol{X}}_{\rm d} + \boldsymbol{K}_v\dot{\boldsymbol{e}} + \boldsymbol{K}_p\boldsymbol{e}) + \hat{\bar{\boldsymbol{H}}}_X\dot{\boldsymbol{X}} + \boldsymbol{W}^T\boldsymbol{\Phi} + \boldsymbol{\mu} \tag{34}$$

where $\boldsymbol{K}_v$ and $\boldsymbol{K}_p$ are positive definite coefficient matrixes. $\boldsymbol{\mu}$ is H_∞ robust control item which is used to eliminate the influence of approximation error.

Substituting (34) into (32) leads to

$$\hat{\bar{\boldsymbol{M}}}_X(\ddot{e} + \boldsymbol{K}_v\dot{\boldsymbol{e}} + \boldsymbol{K}_p\boldsymbol{e}) - \tilde{\boldsymbol{W}}^T\boldsymbol{\Phi} - \Delta\boldsymbol{\delta} + \boldsymbol{\mu} = 0 \tag{35}$$

where $\tilde{\boldsymbol{W}} = \boldsymbol{W}^* - \boldsymbol{W}$ is the weight error matrix of fuzzy neural network.

Denoting $\boldsymbol{Y} = [\boldsymbol{y}_1^T \quad \boldsymbol{y}_2^T] = [\boldsymbol{e}^T \quad \dot{\boldsymbol{e}}^T]^T$, we have:

$$\begin{cases} \dot{\boldsymbol{y}}_1 = \boldsymbol{y}_2 \\ \dot{\boldsymbol{y}}_2 = -\boldsymbol{K}_p\boldsymbol{y}_1 - \boldsymbol{K}_v\boldsymbol{y}_2 + (\ddot{e} + \boldsymbol{K}_v\dot{\boldsymbol{e}} + \boldsymbol{K}_p\boldsymbol{e}). \end{cases} \tag{36}$$

The system state space equations are developed as

$$\dot{\boldsymbol{Y}} = \boldsymbol{A}\boldsymbol{Y} + \boldsymbol{B}\hat{\bar{\boldsymbol{M}}}_X^{-1}(\tilde{\boldsymbol{W}}^T\boldsymbol{\Phi} + \Delta\boldsymbol{\delta} - \boldsymbol{\mu}) \tag{37}$$

where $\boldsymbol{A} = \begin{bmatrix} \boldsymbol{0} & \boldsymbol{I}_{6\times 6} \\ -\boldsymbol{K}_p & -\boldsymbol{K}_v \end{bmatrix}$, $\boldsymbol{B} = \begin{bmatrix} \boldsymbol{0}_{6\times 6} \\ \boldsymbol{I}_{6\times 6} \end{bmatrix}$.

Assumption 1: The approximation error of the system can be regard as external disturbance, and the inertia parameter uncertainty of model varies in a certain range. Then, the system disturbance can be expressed as $\boldsymbol{\varXi} = \hat{\bar{\boldsymbol{M}}}_X^{-1}\Delta\boldsymbol{\delta} \in L_2[0,\infty)$, assuming there is a positive constant D_δ to make $\int_0^\infty \|\hat{\bar{\boldsymbol{M}}}_X^{-1}\Delta\boldsymbol{\delta}\|^2 dt \le D_\delta$.

Robust control item is designed as follow

$$\boldsymbol{\mu} = \hat{\bar{\boldsymbol{M}}}_X \boldsymbol{\varGamma}^{-1}\boldsymbol{B}^T\boldsymbol{P}\boldsymbol{y} \tag{38}$$

where $\boldsymbol{\varGamma} = \boldsymbol{\varGamma}^T$ is H_∞ gain matrix, positive definite matrix $\boldsymbol{P}$ satisfy the Riccati equation

$$\boldsymbol{P}A + \boldsymbol{A}^T\boldsymbol{P} + \boldsymbol{P}\boldsymbol{B}(\frac{1}{\omega^2}\boldsymbol{I}_{12\times12} - 2\boldsymbol{\varGamma}^{-1})\boldsymbol{B}^T\boldsymbol{P} = -\boldsymbol{Q} \tag{39}$$

where ω is disturbance attenuation index, $\boldsymbol{Q}$ is symmetric positive definite matrix.

The weight matrix is updated by the adaptive law as follow

$$\dot{\boldsymbol{W}} = \varLambda^{-1}\boldsymbol{\varPhi}\boldsymbol{y}^T\boldsymbol{P}\boldsymbol{B}\hat{\bar{\boldsymbol{M}}}_X^{-1} \tag{40}$$

where $\varLambda > 0$ is the weight gain coefficient.

In order to demonstrate the stability and H_∞ tracking characteristics of the system, construct a Lyapunov candidate as follow

$$\boldsymbol{V} = \frac{1}{2}\boldsymbol{y}^T\boldsymbol{P}\boldsymbol{y} + \frac{1}{2}\mathrm{tr}(\tilde{\boldsymbol{W}}^T\boldsymbol{\varLambda}\tilde{\boldsymbol{W}}). \tag{41}$$

Differentiating $\boldsymbol{V}$ with respect to time t yields

$$\begin{aligned}\dot{\boldsymbol{V}} =& \frac{1}{2}\dot{\boldsymbol{y}}^T\boldsymbol{P}\boldsymbol{y} + \frac{1}{2}\boldsymbol{y}^T\boldsymbol{P}\dot{\boldsymbol{y}} + \frac{1}{2}\mathrm{tr}(\tilde{\boldsymbol{W}}^T\boldsymbol{\varLambda}\dot{\tilde{\boldsymbol{W}}})\\ =& \frac{1}{2}\left[\boldsymbol{A}\boldsymbol{y} + \boldsymbol{B}\hat{\bar{\boldsymbol{M}}}_X^{-1}(\tilde{\boldsymbol{W}}\boldsymbol{\varPhi} + \Delta\boldsymbol{\delta} - \boldsymbol{\mu})\right]^T\boldsymbol{P}\boldsymbol{y}\\ &+ \frac{1}{2}\boldsymbol{y}^T\boldsymbol{P}\left[\boldsymbol{A}\boldsymbol{y} + \boldsymbol{B}\hat{\bar{\boldsymbol{M}}}_X^{-1}(\tilde{\boldsymbol{W}}\boldsymbol{\varPhi} + \Delta\boldsymbol{\delta} - \boldsymbol{\mu})\right]\\ &+ \mathrm{tr}(\tilde{\boldsymbol{W}}^T\boldsymbol{\varLambda}\dot{\tilde{\boldsymbol{W}}})\\ =& \frac{1}{2}\boldsymbol{y}^T\left[\boldsymbol{P}\boldsymbol{A} + \boldsymbol{A}^T\boldsymbol{P} + \boldsymbol{P}\boldsymbol{B}\left(\frac{1}{\omega^2}\boldsymbol{I}_{3\times3} - 2\boldsymbol{\varGamma}^{-1}\right)\boldsymbol{B}^T\boldsymbol{P}\right]\boldsymbol{y}\\ &- \frac{1}{2}\left(\frac{1}{\omega}\boldsymbol{B}^T\boldsymbol{P}\boldsymbol{y} - \omega\boldsymbol{\varXi}\right)^T\left(\frac{1}{\omega}\boldsymbol{B}^T\boldsymbol{P}\boldsymbol{y} - \omega\boldsymbol{\varXi}\right)\\ &+ \frac{1}{2}\omega^2\boldsymbol{\varXi}^T\boldsymbol{\varXi} \le -\frac{1}{2}\boldsymbol{y}^T\boldsymbol{Q}\boldsymbol{y} + \frac{1}{2}\omega^2\boldsymbol{\varXi}^T\boldsymbol{\varXi}\end{aligned} \tag{42}$$

Integrating (42) over the interval $[0, T_0]$ leads to

$$\boldsymbol{V}(T_0) - \boldsymbol{V}(0) \le -\frac{1}{2}\int_0^{T_0}\boldsymbol{y}^T\boldsymbol{Q}\boldsymbol{y} + \frac{1}{2}\omega^2\int_0^{T_0}\boldsymbol{\varXi}^T\boldsymbol{\varXi}dt. \tag{43}$$

Since $V(T_0) \ge 0$, we have:

$$\frac{1}{2}\int_0^{T_0}\boldsymbol{y}^T\boldsymbol{Q}\boldsymbol{y} \le \boldsymbol{V}(0) + \frac{1}{2}\omega^2\int_0^{T_0}\boldsymbol{\varXi}^T\boldsymbol{\varXi}dt.$$

Therefore, the system tracking errors satisfy H_∞ tracking characteristics of the system.

For $\boldsymbol{\varXi} \in L_2[0,\infty)$, there exist $\eta > 0$ make $\|\boldsymbol{\varXi}\| \le \eta$. From (42) we obtain that

$$\dot{\boldsymbol{V}} \le -\frac{1}{2}\lambda_{\min}(\boldsymbol{Q})\|\boldsymbol{y}\|^2 + \frac{1}{2}\omega^2\eta^2 \tag{44}$$

where $\lambda_{\min}(\cdot)$ represents the minimum value of eigenvalue.

For the arbitrarily small value $\alpha > 0$, we choose

$$\lambda_{\min}(\boldsymbol{Q}) > \frac{\omega^2\eta^2}{\alpha^2} \tag{45}$$

There exist $\beta > 0$, let

$$\dot{\boldsymbol{V}} \le -\beta\|\boldsymbol{y}\|^2 < 0, \quad \forall\|\boldsymbol{y}\| > \alpha \tag{46}$$

Hence, the state variables of system are bounded.

The virtual input force/torque vector $\boldsymbol{\tau}$ is 9-dimensional. The vector $\bar{\boldsymbol{\tau}}$ cannot represent the true input of dual-arm space robot with closed chain. From the preview derivation process, we known that input force/torque of base can be obtained directly. Invoking (25), and (26), the input torques are distributed by the weighted minimum-norm solution

$$\begin{bmatrix}\boldsymbol{\tau}_L\\ \boldsymbol{\tau}_R\end{bmatrix} = \boldsymbol{E}\boldsymbol{\Omega}^T(\boldsymbol{\Omega}\boldsymbol{E}\boldsymbol{\Omega}^T)^{-1}\bar{\boldsymbol{\tau}}_{\mathrm{b}} \tag{47}$$

where $\boldsymbol{E}$ is a diagonal gain matrix.

IV. Numerical Simulation

The dual-arm space robot with two three-degree-of-freedom space manipulator arms is selected to verify the performance of the proposed control scheme. The dual-arm space robot impacted by a spin spacecraft, and form a closed chain system with unstable status in the post-impact phase.

The inertial parameters of composite system are given as: $d_0 = 1.062\,\mathrm{m}$, $d_L = 0.5\,\mathrm{m}$, $d_R = 0.5\,\mathrm{m}$, $l_i = 2\,\mathrm{m}$ ($i = 1, 2, 4, 5$), $l_j = 0.5\,\mathrm{m}$ ($j = 3, 6$). $m_0 = 200\,\mathrm{kg}$, $m_l = 50\,\mathrm{kg}$, $m_i = 10\,\mathrm{kg}$ ($i = 1, 2, 4, 5$), $m_j = 2.5\,\mathrm{kg}$ ($j = 3, 6$). $I_0 = 50\,\mathrm{kg}\cdot\mathrm{m}^2$, $I_l = 20\,\mathrm{kg}\cdot\mathrm{m}^2$, $I_i = 5\,\mathrm{kg}\cdot\mathrm{m}^2$ ($i = 1, 2, 4, 5$), $I_j = 2\,\mathrm{kg}\cdot\mathrm{m}^2$ ($j = 3, 6$). $\psi_1 = 2.791\,\mathrm{rad}$, $\psi_2 = 0.349\,\mathrm{rad}$.

The initial state vector of base in pre-impact phase is

$$\boldsymbol{X} = [0.3\,\mathrm{m}\ \ 0.3\,\mathrm{m}\ \ 0^\circ\ \ 0.3\,\mathrm{m}\ \ 4.1281\,\mathrm{m}\ \ 0^\circ]^T$$

The initial velocity vector of load in pre-impact phase is

$$\dot{\boldsymbol{q}}_l = [-0.4\,\mathrm{m/s}\ \ -0.2\,\mathrm{m/s}\ \ -0.3\,\mathrm{rad/s}]^T$$

The fuzzy neural network is a four-layer network, the number of nodes for each layer is taken as: 12-36-3^{12}-6. And $m = 12$, $n = 3$, $u = 3^{12}$, $s = 6$. The input variables of fuzzy neural network are $\boldsymbol{Y} = [\boldsymbol{e}^T\ \ \dot{\boldsymbol{e}}^T]^T \in \mathbb{R}^{6\times1}$, the center value and base width of Gauss function of ith input variable are $\boldsymbol{c}_i = [-0.5\ \ 0\ \ 0.5]^T$, $b_{ij} = 0.5$ respectively, the weight matrix $\boldsymbol{W}$ are adjusted by $\dot{\boldsymbol{W}}$. The nominal models of composite system are taken as: $\hat{\bar{\boldsymbol{M}}}_X = 0.8\bar{\boldsymbol{M}}_X$, $\hat{\bar{\boldsymbol{H}}}_X = 0.8\bar{\boldsymbol{H}}_X$. The interrelated control parameters are taken as: $\boldsymbol{K}_v = 2\boldsymbol{I}_{6\times6}$, $\boldsymbol{K}_p = \boldsymbol{I}_{6\times6}$, $\omega = 0.05$, $\boldsymbol{Q} = 12\boldsymbol{I}_{12\times12}$, $\boldsymbol{\varGamma} = 0.2\boldsymbol{I}_{6\times6}$.

Instantaneous time after collision is regard as initial time. In order to hold up the collision between dual-arm space robot and target. There is no input torques during two-second response time. The simulation results are shown in Figs. 4–9. Figs. 4 and 5 show the tracking curves of the base position and attitude. Figs. 6 – 8 show the tracking curves of the load position and attitude. The collision will lead to disturbed motion for system, the composite system is an unstable closed chain system in the post-impact phase, it is harm for the precision equipments.

After two-second response time, the output matrix of system reach the states as

$\boldsymbol{X} = [0.3057\,\mathrm{m}\ \ 0.2942\,\mathrm{m}\ \ 1.28^\circ\ \ -0.0779\,\mathrm{m}\ \ 3.8946\,\mathrm{m}-12.84^\circ]^T$

Using the proposed control scheme can achieve the goal of calm motion. Closed chain system restore to the initial state and keep stable. Fig. 9 is the motion process simulation

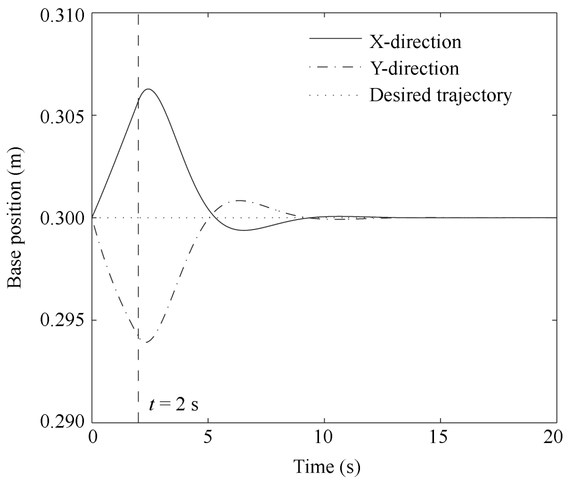

Fig. 4. Time history of base position after impact.

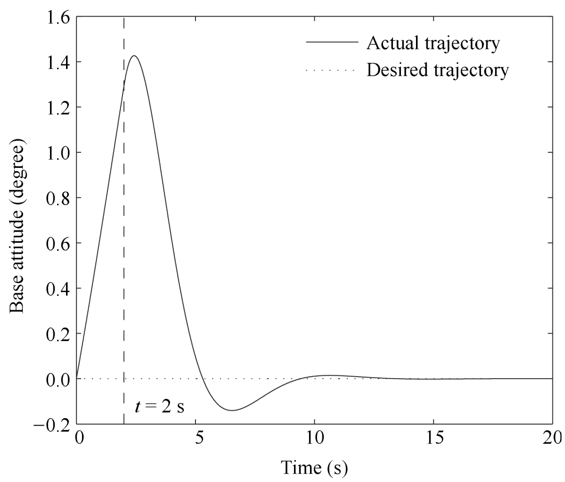

Fig. 5. Time history of base attitude after impact.

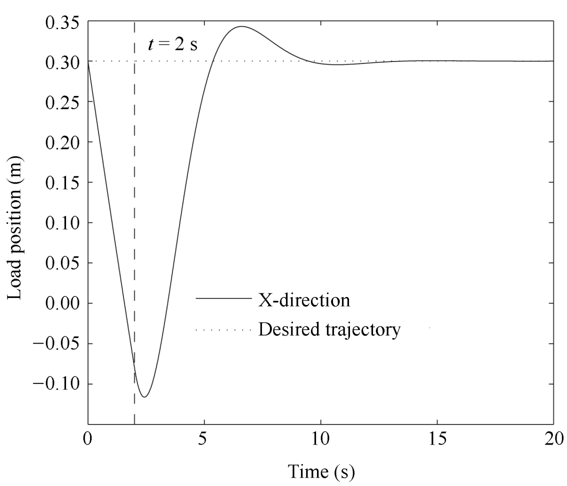

Fig. 6. Time history of load position in the x-direction after impact.

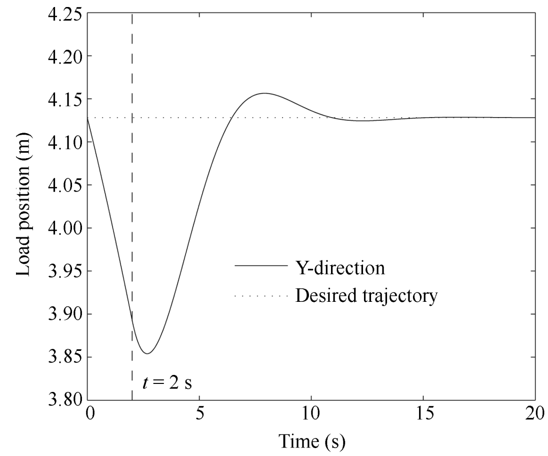

Fig. 7. Time history of load position in the y-direction after impact.

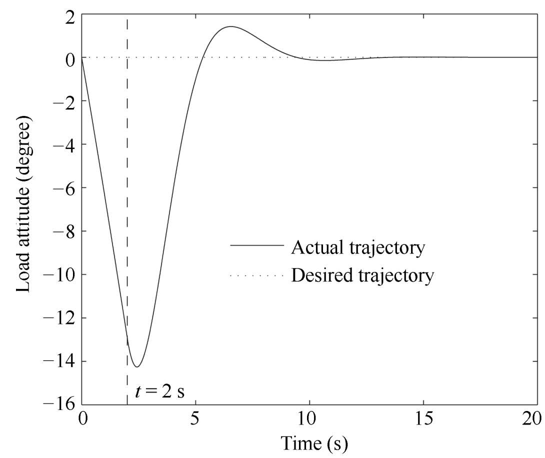

Fig. 8. Time history of load attitude after impact.

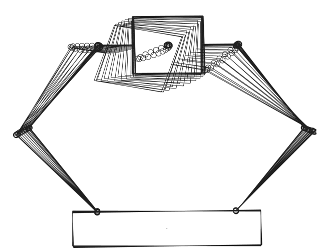

Fig. 9. Motion of the closed chain system after impact.

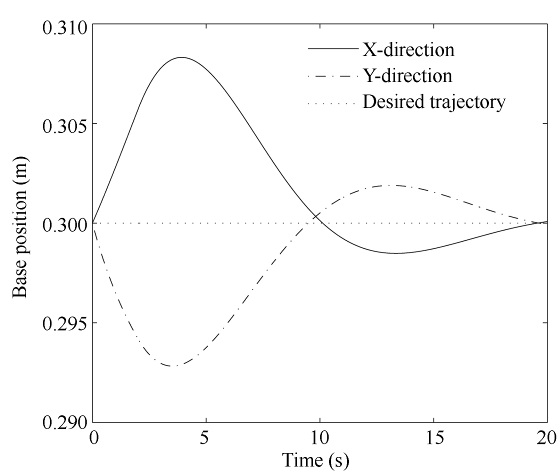

Fig. 10. Time history of base position without compensation control.

diagram of closed chain system which shows the movement is restrained by closed-loop.

To show the performance of the proposed control scheme, a comparison experiment is carried out which close the compensation control. The simulation result are shown in Figs. 10 – 14. Figs. 10 and 11 show the tracking curves of the base position

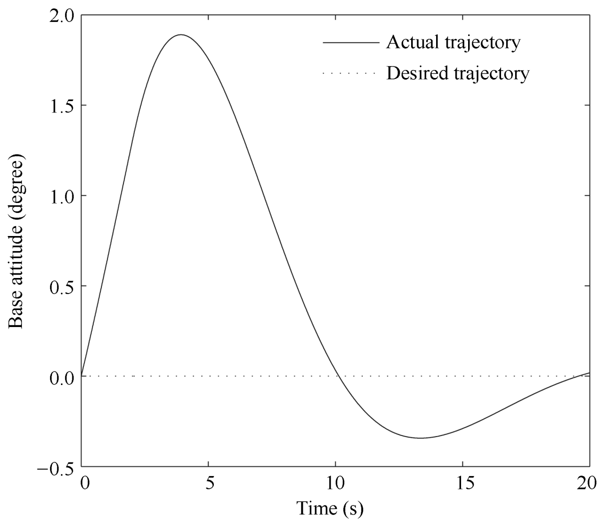

Fig. 11. Time history of base attitude without compensation control.

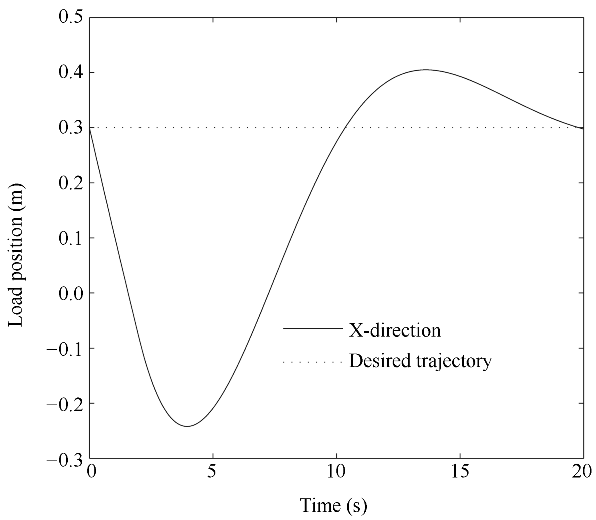

Fig. 12. Time history of load position in the x-direction without compensation control.

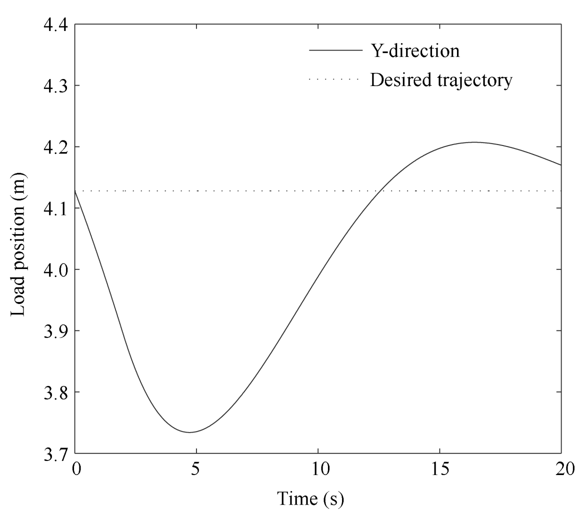

Fig. 13. Time history of load position in the y-direction without compensation control.

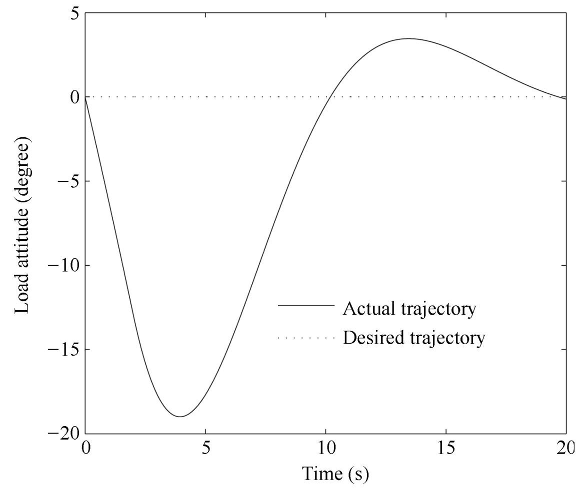

Fig. 14. Time history of load attitude without compensation control.

and attitude. Figs. 12–14 show the tracking curves of the load position and attitude. From the observation of simulation results, in the condition of uncertain inertial parameters, the control performance is poor. Control system cannot achieve control objective by closing the compensation control.

V. Conclusion

The dynamic models of dual-arm space robot and target spacecraft are established by multi-body theory. With the theorem of impulse and force transfer law, the response of dual-arm space robot system impacted by a spin spacecraft is analyzed. The closed chain system model is derived by the constraints of closed-loop geometry and kinematics. In order to accomplish calm motion control for composite system, the recurrent fuzzy neural network control scheme is designed, the control method with H_∞ tracking characteristic. The composite system is unstable in the post-impact phase. The proposed control method inhibits the rolling trend of whole system and remarkable tracking performance is shown in simulation results. The control scheme dispense with accurate system model or linear parameterization of the system dynamic equations.

References

[1] A. Flores-Abad, O. Ma, K. Pham, and S. Ulrich, “A review of space robotics technologies for on-orbit servicing,” *Progress in Aerospace Sciences*, vol. 68, no. 8, pp. 1–26, Jul. 2014.

[2] P. Zarafshan and A. A. Moosavian, “Manipulation control of a flexible space free flying robot using fuzzy tuning approach,” *International Journal of Robotics*, vol. 5, no. 2, pp. 9–18, Jan 2015.

[3] J. Cheng and L. Chen, “Coordinated robust control based on extended state observer of dual-arm space robot with closed chain for transferring a target,” *Proceedings of the Institution of Mechanical Engineers Part G Journal of Aerospace Engineering*, vol. 232, no. 13, pp. 2489–2498, Oct. 2018.

[4] S. Jia, Y. Jia, S. Xu, and H. Quan, “Maneuver and active vibration suppression of free-flying space robot,” *IEEE Transactions on Aerospace & Electronic Systems*, vol. 54, no. 3, pp. 1115–1134, Jun. 2018.

[5] P. Huang, B. Liu, and F. Zhang, “Configuration maintaining control of three-body ring tethered system based on thrust compensation,” *Acta Astronautica*, vol. 123, pp. 37–50, Jul. 2016.

[6] R. Boumans and C. Heemskerk, “The european robotic arm for the international space station,” *Robotics & Autonomous Systems*, vol. 23, no. 1-2, pp. 17–27, Jun. 1998.

[7] M. A. Diftler, J. S. Mehling, M. E. Abdallah, and N. A. Radford, "Robonaut 2 - the first humanoid robot in space," in *Proc. IEEE International Conference on Robotics and Automation*, May 2011, pp. 2178−2183.

[8] P. Huang, F. Zhang, Z. Meng, and Z. Liu, "Adaptive control for space debris removal with uncertain kinematics, dynamics and states," *Acta Astronautica*, vol. 128, pp. 416−430, Dec. 2016.

[9] Y. Xu and H. Y. Shum, "Dynamic control and coupling of a free-flying space robot system," *Journal of Robotic Systems*, vol. 11, no. 7, pp. 573−589, Jul. 1994.

[10] I. S. Paraskevas and E. Papadopoulos, "Parametric sensitivity and control of on-orbit manipulators during impacts using the centre of percussion concept," *Control Engineering Practice*, vol. 47, pp. 48−59, 2016.

[11] J. Liang and L. Chen, "Improved nonlinear feedback control for freefloating space-based robot with time-delay based on predictive and approximation of taylor series," *Acta Aeronautica et Astronautica Sinica*, vol. 33, no. 1, pp. 163−169, Oct. 2012.

[12] O. Parlaktuna and M. Ozkan, "Adaptive control of free-floating space manipulators using dynamically equivalent manipulator model," *Robotics & Autonomous Systems*, vol. 46, no. 3, pp. 185−193, Mar. 2004.

[13] M. W. Walker and L. B. Wee, "Adaptive control of space-based robot manipulators," *IEEE Transactions on Robotics & Automation* , vol. 7, no. 6, pp. 828−835, Dec. 1992.

[14] Z. Vafa and S. Dubowsky, "The kinematics and dynamics of space manipulators: the virtual manipulator approach," *International Journal of Robotics Research*, vol. 9, no. 4, pp. 3−21, Aug. 1990.

[15] Y. Nakamura and R. Mukherjee, "Exploiting nonholonomic redundancy of free-flying space robots," *IEEE Transactions on Robotics & Automation*, vol. 9, no. 4, pp. 499−506, Jul. 1993.

[16] D. Wang, P. Huang, and Z. Meng, "Coordinated stabilization of tumbling targets using tethered space manipulators," *IEEE Transactions on Aerospace & Electronic Systems*, vol. 51, no. 3, pp. 2420−2432, Jul. 2015.

[17] P. Huang, D. Wang, Z. Meng, F. Zhang, and J. Guo, "Adaptive post-capture backstepping control for tumbling tethered space robot-target combination," *Journal of Guidance Control & Dynamics*, vol. 39, no. 1, pp. 150−156, 2015.

[18] P. Huang, D. Wang, Z. Meng, and F. Zhang, "Impact dynamic modelling and adaptive target capturing control for tethered space robots with uncertainties," *IEEE/ASME Transactions on Mechatronics*, vol. 21, no. 5, pp. 2260−2271, Oct. 2016.

[19] A. F. Abad, W. Zheng, O. Ma, "Optimal control of space robots for capturing a tumbling object with uncertainties," *Journal of Guidance, Control & Dynamics*, vol. 37, no. 6, pp. 2014−2017, Dec. 2014.

[20] G. Rekleitis and E. Papadopoulos, "On-orbit cooperating space robotic servicers handling a passive object," *IEEE Transaction on Aerospace and Electronic System*, vol. 51, no. 2, Apr. 2015, pp. 803−814.

[21] T. Narikiyo, M. Ohmiya, T. Narikiyo, and M. Ohmiya, "Control of a planar space robot: Theory and experiments," *Control Engineering Practice*, vol. 14, no. 8, pp. 875−883, Aug. 2006.

[22] J. Cheng and L. Chen, "Decentralized adaptive neural network stabilization control and vibration suppression of flexible robot manipulator during capture a target," in *Proc. the 66th International Astronautical Congress*, 2015.

[23] V. Dubanchet, D. Saussié, D. Alazard, and C. Berard, "Modeling and control of a space robot for active debris removal," *CEAS Space Journal*, vol. 7, no. 2, pp. 203−218, Jun. 2015.

[24] H. Patolia, P. Mani Pathak, and S. C. Jain, "Trajectory control of a dual-arm planar space robot with little attitude disturbance," *Simulation*, vol. 87, no. 3, pp. 188−204, Mar. 2011.

[25] Z. Chen and L. Chen, "Compensation control for grasped object of dualarm space robot with closed-chain based on radial basis function neural network," *Journal of Mechanical Engineering*, vol. 47, no. 7, pp. 38−44, Apr. 2011.

[26] S. V. Shah, S. Inna, and K. M. Arun, "Reactionless path planning strategies for capture of tumbling objects in space using a dual-arm robotic system," in *Proc. AIAA Guidance, Navigation, and Control Conference*, Aug. 2013, pp. 1−12.

[27] R. Ballini and F. Gomide, "Recurrent fuzzy neural computation: Modeling, learning and application," in *Proc. IEEE International Conference on Fuzzy Systems*, Jul. 2010, pp. 1−6.

[28] S. I. Han and J. M. Lee, "Recurrent fuzzy neural network backstepping control for the prescribed output tracking performance of nonlinear dynamic systems." *ISA Transactions*, vol. 53, no. 1, pp. 33−43, Jan. 2014.

[29] B. S. Chen, C. H. Lee, and Y. C. Chang, "H1 tracking design of uncertain nonlinear siso systems: adaptive fuzzy approach," *IEEE Transactions on Fuzzy Systems*, vol. 4, no. 1, pp. 32−43, Feb. 1996.

[30] A. Rubaai, "Direct adaptive fuzzy control design achieving h1 tracking for high performance servo drives," *IEEE Transactions on Energy Conversion*, vol. 14, no. 4, pp. 1199−1208, Dec. 1999.

[31] S. A. A. Moosavian and E. Papadopoulos, "On the control of space free-flyers using multiple impedance control," in *Proc. IEEE International Conference on Robotics and Automation*, vol. 1, Apr. 1997, pp. 853−858.

[32] F. L. Lewis, K. Liu, and A. Yesildirek, "Neural net robot controller with guaranteed tracking performance," *IEEE Transactions on Neural Networks*, vol. 6, no. 3, pp. 703−715, May. 1995.

[33] B. A. M. Wakileh and K. F. Gill, "Robot control using self-organizing fuzzy logic," *Computers in Industry*, vol. 15, no. 3, pp. 175−186, 1990.

[34] C. T. Lin and C. S. G. Lee, "Reinforcement structure/parameter learning for neural-network-based fuzzy logic control systems," *IEEE Transactions on Fuzzy Systems*, vol. 2, no. 1, pp. 72−84, Feb. 1994.

[35] F. Sun, L. Li, H.-X. Li, and H. Liu, "Neuro-fuzzy dynamic-inversionbased adaptive control for robotic manipulators—discrete time case," *IEEE Transactions on Industrial Electronics*, vol. 54, no. 3, pp. 1342− 1351, Jun. 2007.

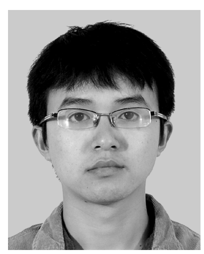

Jing Cheng is currently a Postdoc Fellow of School of Aerospace Engineering at Tsinghua University, Beijing, China. He received the Ph.D. degree from Fuzhou University, China in 2017. His research interests include multi-body dynamics, man-machine interaction, dynamics and control of space robot systems and vibration control.

Li Chen received the B.S. degree in mathematics and mechanics from Jilin University, Jilin, China, in 1984 and the M.S. degree in general mechanics from Northeastern University, China, in 1994 and the Ph.D. degree in general mechanics from Shanghai Jiao Tong University, China, in 1997. He is currently a Professor with the School of Mechanical Engineering and Automation, Fuzhou University, Fujian, China. His research interests include space robot system dynamics and control, multi-body dynamics, nonlinear vibration.

From 2004 to 2005, he was a visiting professor in the robotics laboratory of Canadian Laval University. He is Vice Chairman of Mechanical institute of Fujian province and committee member of the Chinese Society of Theoretical and Applied Mechanics. He has authored or co-authored more than 300 scientific papers published in journals and conference proceedings.